Atmospheric transmission at submillimetre wavelengths from Mauna Kea

D. A. Naylor,[1]★ G. R. Davis,[2] B. G. Gom,[3] T. A. Clark[4] and M. J. Griffin[5]

[1]*Department of Physics, University of Lethbridge, Lethbridge, Alberta T1K 3M4, Canada*
[2]*Institute of Space and Atmospheric Studies, University of Saskatchewan, Saskatoon, Saskatchewan S7N 5E2, Canada*
[3]*Joint Astronomy Centre, 660 N. A'ohōkū Place, University Park, Hilo, Hawaii 96720, USA*
[4]*Department of Physics and Astronomy, University of Calgary, Calgary, Alberta T2N 1N4, Canada*
[5]*Department of Physics, Queen Mary and Westfield College, Mile End Road, London E1 4NS*

ABSTRACT

The submillimetre atmospheric transmission spectrum above Mauna Kea has been measured at a resolution of $0.005 \, \mathrm{cm}^{-1}$ (150 MHz) with a Fourier transform spectrometer at the James Clerk Maxwell Telescope, using the Sun as a source. Column abundances of O_2, H_2O and O_3 determined from these spectra are found to be in excellent agreement with independent measurements. The derived column abundances have been used as inputs to the atmospheric spectral modelling program FASCOD. The synthetic transmission spectrum is found to be in excellent agreement with the measured spectrum, and provides a template for submillimetre observations from the JCMT.

Key words: atmospheric effects – instrumentation: interferometers – techniques: spectroscopic.

1 INTRODUCTION

The rapid growth of submillimetre astronomy in recent years is primarily due to technological advances which have led to the development of sensitive detector systems and spectrometers. In contrast with heterodyne receivers, which offer high spectral resolution but limited spectral range, spectrometers based on incoherent detection (Fourier transform, Fabry–Perot, grating) offer broad spectral coverage at intermediate resolution. This combination of properties is ideally suited to the study of planetary atmospheres and bright extragalactic objects which have linewidths greater than the bandwidth of heterodyne receivers.

In 1990 February, an existing classical Michelson interferometer (Naylor & Clark 1986), modified to operate at submillimetre wavelengths, was used to measure the atmospheric transmission above Mauna Kea (Naylor et al. 1991) in order to determine the feasibility of conducting broad-band spectroscopic observations from the James Clerk Maxwell Telescope (JCMT). These encouraging results provided the impetus for developing a polarizing Fourier transform spectrometer (FTS) (Naylor, Clark & Davis 1994a) which used the JCMT facility bolometer UKT14 (Duncan et al. 1990) as the detecting element.

While the initial observing runs proved the FTS design concept, as evidenced by the first incoherent detection of the CO $J = 6 \rightarrow 5$ transition at $23.0651 \, \mathrm{cm}^{-1}$ from the Orion molecular cloud (Naylor et al. 1993), it was readily apparent that UKT14 was limiting the performance of the FTS. UKT14 was designed for astronomical photometry (using phase-sensitive detection synchronized to the chopping secondary mirror of the JCMT), but,

when used as a spectroscopic detector with the FTS, several problem areas were encountered: electrical pickup at the detector, extreme microphonic sensitivity of the dewar, and the presence of several resonant optical cavities within the dewar which produced spectral fringing (Naylor et al. 1994b). Furthermore, since UKT14 contained a single bolometer, only one half of the radiation processed by the polarizing FTS was detected.

To address these issues, a dual-polarization bolometer detector system (Naylor et al. 1999) has been developed for use with the polarizing FTS at the JCMT. The system employs a fully differential electronic design which virtually eliminates common mode electrical noise from the often hostile telescope environment. In addition, the optical design minimizes the background radiant loading on the bolometer elements and the occurrence of resonant optical cavities.

In this paper we present atmospheric transmission spectra obtained using this new detector system, in conjunction with the FTS, over the spectral range 350–1100 μm. These spectra were obtained using the Sun as the source, which provided high signal-to-noise ratio data in a short observing time. By comparison, spectra obtained by emission techniques (Matsuo, Sakamoto & Matsushita 1998; Serabyn et al. 1998; Matsushita et al. 1999) require both long integration times and a priori knowledge of the atmospheric temperature profile. While the transmission technique yields superior absorption-line profiles, the accuracy of the continuum calibration is limited by the uncertainty in the solar brightness temperature at these wavelengths. Furthermore, use of the Sun as a source restricts the region of the atmosphere that can be studied.

The observations and analysis are described in Sections 2 and 3 respectively. In Section 4 we derive column abundances of O_2, H_2O and O_3, and compare these with independent measurements.

★ E-mail: naylor@uleth.ca

Table 1. Interferometer characteristics.

Interferometer	Martin–Puplett, double input, double output	
Scan mode	Rapid scan, maximum scan time $\sim$60 s	
Resolution	.005 cm^{-1}, 150 MHz ($R \sim 6 \times 10^3$ @ 30 cm^{-1})	
Polarizers	Free-standing tungsten wire (10-μm diameter, 20-μm period)	
Detectors	2 NTD bolometers, 0.3 K	
Beamwidth	$\sim$7–19 arcsec (FWHM)	
Spectral Bands	1100 μm	8.1–10.4 cm^{-1} (243–312 GHz)
	850 μm	11.2–12.1 cm^{-1} (336–363 GHz)
	750 μm	12.9–13.9 cm^{-1} (387–417 GHz)
	450 μm	21.1–23.5 cm^{-1} (633–705 GHz)
	351 μm	26.2–29.2 cm^{-1} (786–876 GHz)
	349 μm	28.8–29.9 cm^{-1} (864–897 GHz)
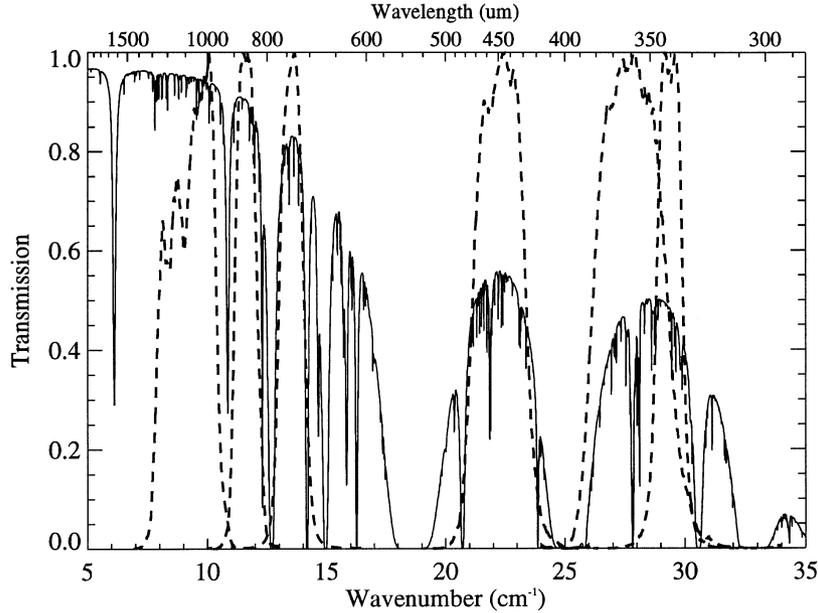
Figure 1. Available filter bands (broken curves) superimposed on zenith model atmospheric transmission spectrum above Mauna Kea for 0.5-mm precipitable water vapour (pwv), corresponding to excellent observing conditions.

2 OBSERVATIONS

The observations reported here were obtained on the morning of 1998 May 26. The polarizing FTS was mounted at the west Nasmyth focus of the JCMT and fed by an *f*/16 beam from the plane tertiary mirror of the JCMT, in a manner identical to the SCUBA input feed optics (Holland et al. 1999), by a small shift in the secondary mirror position. The interferometer was operated in rapid-scan mode, producing modulation frequencies at the detector of 20–50 Hz. Important instrumental parameters are given in Table 1.

Atmospheric transmission spectra were obtained using the Sun as a source. The extended size of the Sun required that the interferometer be operated in single-beam mode, with one input port viewing the Sun while the second input port viewed a cold blackbody source (an Eccosorb[1] AN 74 cone immersed in a liquid N_2 dewar). Spectra were acquired in pairs: two spectra on the centre of the Sun were immediately followed by two from a sky position 2000 arcsec in azimuth from the centre of the Sun (about one solar radius from the limb of the Sun). This approach, in which individual spectra were obtained every minute, minimized differences in atmospheric transmission between solar and background measurements.

[1] Eccosorb: Emerson & Cuming, 604W 182 St, Gardena, CA 90248, USA.

Table 2. Summary of observations.

Spectral band	Number of spectrum pairs	Airmass
1100 μm	2	1.71
850 μm	2	1.64
750 μm	2	1.60
450 μm	2	1.53
351 μm	2	1.47

The detector system contains a six-position filter wheel. The six bandpass filters used in these observations are listed in Table 1, and their normalized spectral profiles are shown in Fig. 1. The bandpass of each filter is designed to match the atmospheric windows. Spectra were obtained in each of the six filter bands at a resolution of 0.005 cm^{-1} (150 MHz). For each filter the focal plane aperture within the dewar was selected to match the diffraction-limited beamwidth of the telescope, which varies from 7 arcsec at 350 μm to 19 arcsec at 1100 μm. Although solar limb scanning has revealed that the actual beam pattern is both distorted and extended (Lindsey & Roellig 1991; Clark et al. 1992), the effect of this non-Gaussian beam on measurements taken at the centre of the Sun is negligible. The observations are summarized in Table 2.

3   ANALYSIS

In rapid-scan mode, interferograms are recorded at a rate of $4 \, \mathrm{kB \, s^{-1}}$ which necessitates a high level of automation in the subsequent data analysis. Raw interferograms are first screened for quality. A procedure written in IDL[2] automatically detects and allows for the interactive removal of noise spikes, in particular the ubiquitous cosmic rays which contaminate roughly 1 in every 10 interferograms. Once cleaned, standard Fourier transform spectroscopic analysis techniques are applied to the raw data. The interferogram is heavily oversampled (8 and 24 times at wavelengths of 350 and $1100 \, \mu\mathrm{m}$, respectively) to allow for the application of a digital filter prior to phase correction. Since the optical elements in the spectrometer and detector produce negligible dispersion over the narrow spectral range of interest, a linear phase correction, determined by weighting phase values obtained from a short, double-sided interferogram by the amplitude of the corresponding spectral point, is applied to each interferogram before Fourier transformation (Forman, Steel & Vanasse 1966).

The measured signal when observing the Sun can be expressed as

$$S_{\mathrm{Sun}}(\nu) = R(\nu)[\eta B(\nu, T_{\mathrm{Sun}}) \, \mathrm{e}^{-\tau(\nu)} + \eta B(\nu, T_{\mathrm{sky}})(1 - \mathrm{e}^{-\tau(\nu)})$$
$$+ (1 - \eta)B(\nu, T_{\mathrm{amb}}) - J'(\nu)], \tag{1}$$

where ν is the frequency, $R(\nu)$ is the responsivity of the spectrometer, η is the coupling efficiency of the telescope to an extended astronomical source, $B(\nu, T)$ is the Planck blackbody function at temperature T, and $\tau(\nu)$ is the atmospheric optical depth. The first term represents the power received from the Sun, the second term represents power received from the emitting atmosphere, the third term represents power received from ambient temperature surfaces of the telescope, and the final term, $J'(\nu)$, represents the total power received through the second port of the FTS which is differenced in the interferometric measurement.

For observations at the background position the measured signal, $S_{\mathrm{sky}}(\nu)$, can be expressed as

$$S_{\mathrm{sky}}(\nu) = R(\nu)[\eta_i J_i(\nu) \, \mathrm{e}^{-\tau(\nu)} + \eta B(\nu, T_{\mathrm{sky}})(1 - \mathrm{e}^{-\tau(\nu)})$$
$$+ (1 - \eta)B(\nu, T_{\mathrm{amb}}) - J'(\nu)], \tag{2}$$

where the first term represents the power received from other external sources (e.g. cosmic, galactic and zodiacal). In general these sources could have differing coupling efficiencies (η_i) and non-thermal emission spectra, but in practice their contribution to the total power received is negligible with respect to that received from the Sun (Serabyn et al. 1998). Assuming that the atmospheric temperature and opacity remain constant during each spectral pair, the difference between the source and background spectra is

$$S_{\mathrm{Sun}}(\nu) - S_{\mathrm{sky}}(\nu) = R(\nu)\eta B(\nu, T_{\mathrm{Sun}}) \, \mathrm{e}^{-\tau(\nu)}, \tag{3}$$

which can be inverted to yield the atmospheric transmission, $t(\nu)$:

$$t(\nu) = \mathrm{e}^{-\tau_\nu} = \frac{S_{\mathrm{Sun}}(\nu) - S_{\mathrm{sky}}(\nu)}{R(\nu)\eta B(\nu, T_{\mathrm{Sun}})}. \tag{4}$$

The responsivity, $R(\nu)$, of the spectrometer was determined by placing ambient and cooled blackbody sources in one input port of the FTS:

$$R(\nu) = \frac{S_{\mathrm{amb}}(\nu) - S_{\mathrm{cold}}(\nu)}{B(\nu, T_{\mathrm{amb}}) - B(\nu, T_{\mathrm{cold}})}. \tag{5}$$

[2] IDL: Research Systems Inc., 2995 Wilderness Place, Suite 203, Boulder, CO 80301, USA.

The telescope coupling efficiency, η, was taken from Matthews (1999). For the solar temperature, $T_{\mathrm{Sun}}(\nu)$, we have adopted the VAL C model of Vernazza, Avrett & Loeser (1981), which increases smoothly from 4835 K at $350 \, \mu\mathrm{m}$ to 6100 K at $1100 \, \mu\mathrm{m}$.

Four sources of error contribute to the uncertainty in the derived transmission (equation 4). The uncertainty in the spectral responsivity determination is estimated to be ~2 per cent and that in the telescope coupling efficiency is ~5 per cent. The solar temperature is not well constrained by observations at these wavelengths, and we estimate the uncertainty in the VAL C model to be ~8 per cent. Finally, based on our experience with UKT14 in which the detector responsivity was slightly degraded under solar loading (Davis et al. 1997), we chose in the present measurements to operate the bolometers at a higher bias to minimize this effect. Based on the constancy of the DC voltage developed across the bolometer when viewing the Sun or background positions, and the absence of any observable non-linear features in the resulting spectra, we estimate the reduction in the spectral responsivity under solar loading to be small in comparison with the uncertainty in the solar temperature. The combined uncertainty in the transmission is therefore estimated to be ~10 per cent.

4   RESULTS

The derived transmission spectra between 350 and $1100 \, \mu\mathrm{m}$ are shown in the upper traces of Figs 2–6. Virtually all of the features seen in these spectra are due to O_2, H_2O and O_3. We have analysed these spectra to retrieve column abundances for these three species.

Two magnetic dipole transitions of O_2, the 5_4–3_3 and 5_5–3_4 lines which occur at 23.862 946 and 27.824 108 cm^{-1} respectively (Figs 5 and 6), provide an independent check of the relative calibration of the transmission spectra. Since these lines are saturated, the O_2 column abundance, u, has been determined from the measured equivalent widths, W:

$$u = \frac{W^2}{4S\alpha_{\mathrm{L}}}, \tag{6}$$

where S is the line strength and α_{L} is the Lorentz width. These parameters were taken from the HITRAN96 data base (Rothman et al. 1998) and corrected for the mean atmospheric temperature and pressure of 280 K and 312 mb. Using these two lines the vertical O_2 column abundance was found to be $2.50 \pm 0.38 \times 10^{24}$ molecule cm^{-2}, which agrees well with the known value of 2.676×10^{24} molecule cm^{-2} for a base pressure of 625 mb.

Although the filter bands are specifically designed to avoid the deep H_2O lines, there is sufficient signal in the 850-$\mu\mathrm{m}$ band, when observing the Sun, to allow quantitative measurements of the 5_{15}–4_{22} H_2O transition at 10.845 934 cm^{-1} (Fig. 3). The vertical column abundance of H_2O determined from this line using equation (5) is $1.97 \pm 0.20 \times 10^{21}$ molecule cm^{-2}, corresponding to 0.59 ± 0.06 mm precipitable water vapour (pwv). This value is in excellent agreement with an independent measurement by the Caltech Submillimetre Observatory (CSO) heterodyne radiometer (Chamberlin & Bally 1994) operating at 225 GHz: the measured zenith opacity at the time of these observations was 0.044, corresponding to 0.56 mm pwv (Davis et al. 1997, equation 3).

The O_3 column abundance can be determined from the numerous O_3 lines that pervade the submillimetre spectral region. We have used 25 isolated lines in the 450-$\mu\mathrm{m}$ band (Fig. 5) to determine the column abundance. Since these lines are not
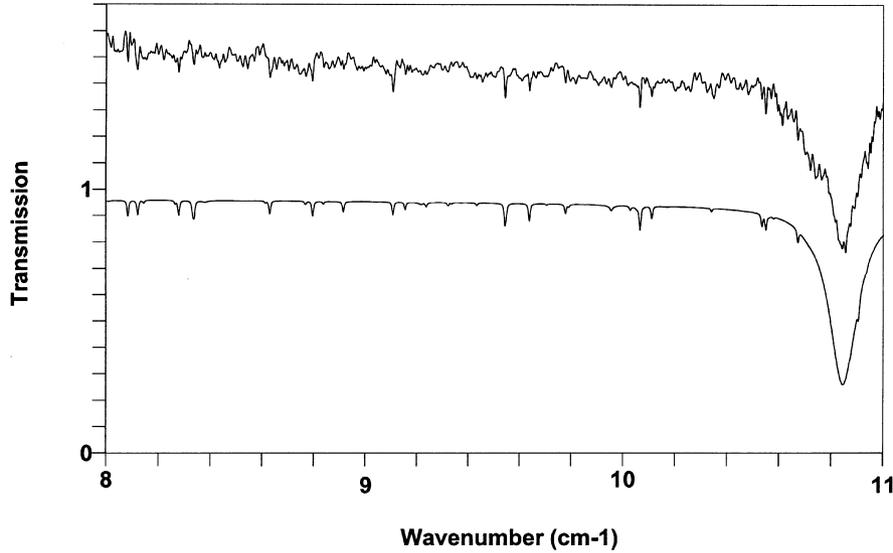
Figure 2. Theoretical atmospheric transmission spectrum (lower trace) compared with measured atmospheric transmission spectrum (upper trace) offset by 0.5 for the 1100-µm filter band (240–330 GHz).
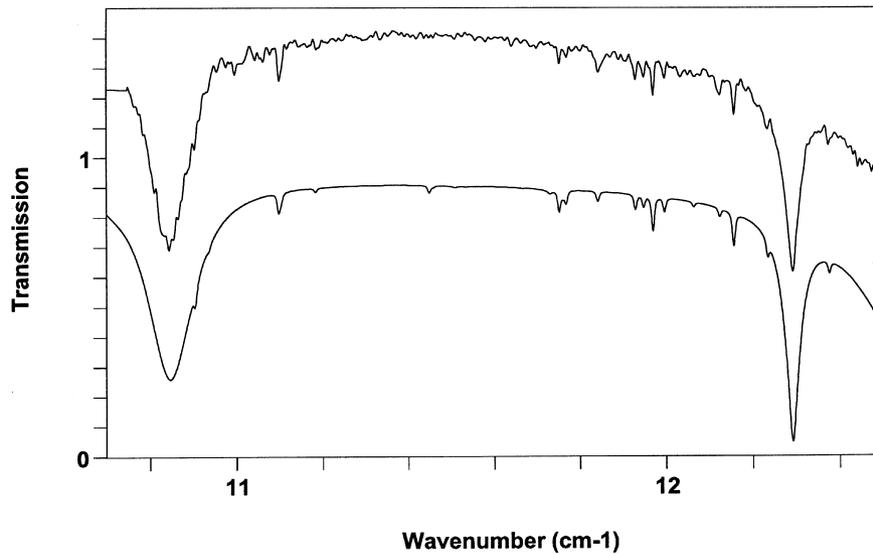
Figure 3. As Fig. 2 for the 850-µm filter band (321–375 GHz).

resolved by the spectrometer, retrieval of the O_3 vertical profile is not possible. We have therefore compared the measured line: continuum ratios of all 25 lines against those calculated from a set of model spectra. The synthetic spectra were calculated using FASCOD (Anderson et al. 1996) in conjunction with its internal tropical atmospheric model. While retaining the O_3 vertical distribution profile in this model, the O_3 column abundance was varied and the value that produced best agreement with the measured line: continuum ratios was determined. The O_3 column abundance averaged over the 25 lines is $7.44 \pm 0.03 \times 10^{18}$ molecule cm^{-2}. This value is in excellent agreement with an independent O_3 measurement of 7.39×10^{18} molecule cm^{-2}, recorded by the Dobson spectrophotometer at the nearby Mauna Loa Observatory (http://mloserv.mlo.hawaii.gov) some three hours later. In contrast with recent emission measurements by Serabyn et al. (1998) and Matsushita et al. (1999), the high level

of agreement between O_3 abundance values obtained in this work is a direct result of accurately modelling the stratospheric temperature profile.

The O_3 line measurements also provide a useful means of measuring the spectroscopic performance of the FTS. The measured lines are symmetric with widths of $0.007\,cm^{-1}$, which implies an instrumental spectral resolution of $0.005\,cm^{-1}$ as designed. Furthermore, the wavenumber accuracy, as determined from a statistical analysis of the 52 lines measured with both detectors, is $0.0002\,cm^{-1}$ (6 MHz) rms.

The atmospheric transmission spectrum corresponding to the column abundances determined above for O_2, H_2O and O_3 calculated using FASCOD, as described above, is shown in the lower traces of Figs 2–6. There is seen to be excellent agreement between the measured and model spectra. Fig. 7 shows an expanded region of the 350-µm window and demonstrates the
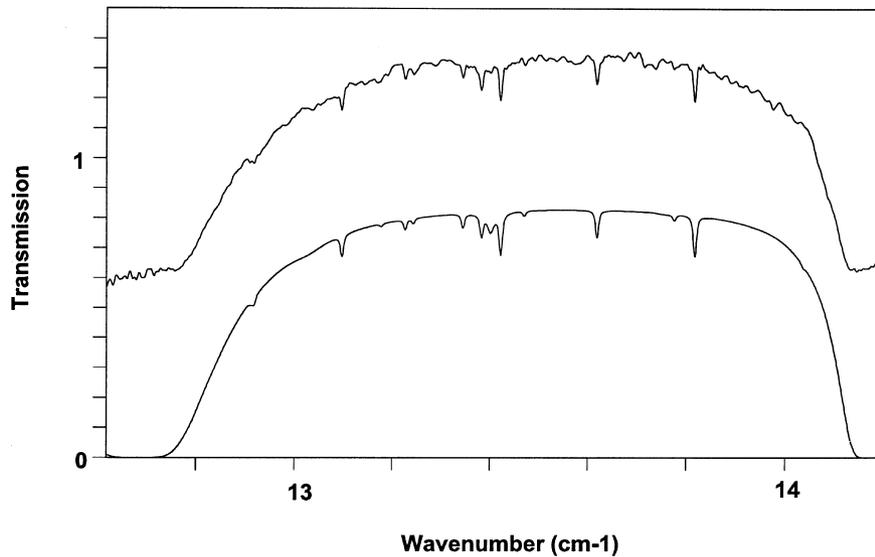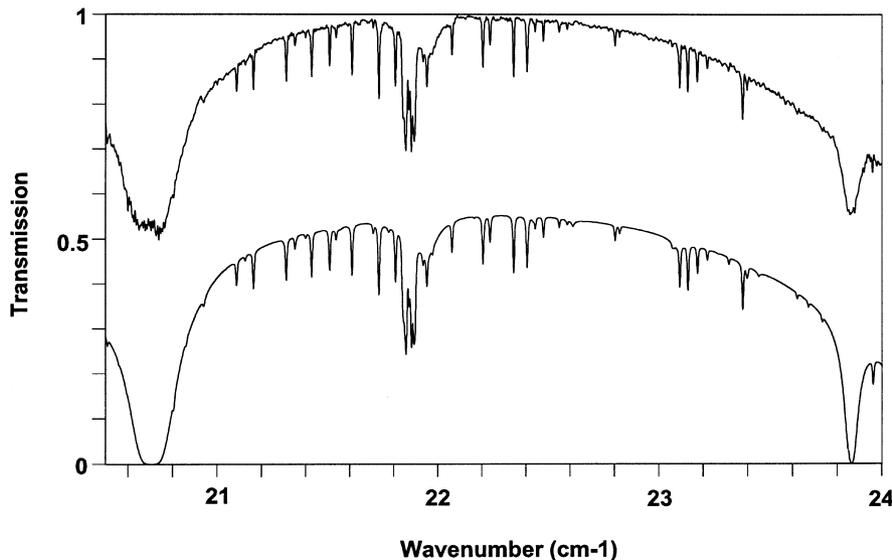
Figure 4. As Fig. 2 for the 750-μm filter band (378–426 GHz).

Figure 5. As Fig. 2 for the 450-μm filter band (615–720 GHz).

high degree of agreement in a complex region that contains a strong O_2 line and a manifold of O_3 transitions.

A major uncertainty in this spectral region is the continuum absorption by H_2O. Although recent atmospheric emission measurements have constrained this contribution to the opacity (Matsuo et al. 1998; Serabyn et al. 1998; Matsushita et al. 1999), the calibration uncertainty of the transmission spectra reported here precludes us from further constraining the continuum absorption. We have therefore used the internal FASCOD continuum parametrization in the present synthesis.

5   CONCLUSION

The submillimetre atmospheric transmission spectrum above Mauna Kea has been measured with a resolution of $0.005\,\mathrm{cm}^{-1}$ using the Sun as a source. Column abundances of O_2, H_2O and O_3

have been determined and are in excellent agreement with independent measurements. These abundances have been used to calculate a synthetic transmission spectrum which agrees well with the measured spectrum within the calibration uncertainty of 10 per cent. The calibration uncertainty could be reduced by using the Moon as a source, since its submillimetre brightness temperature is more accurately known.

Validation of the FASCOD atmospheric model enables its use in planning astronomical observations at submillimetre wavelengths. This will be particularly useful as heterodyne receivers are developed for the 350- and 450-μm windows in which the density of O_3 lines is higher.
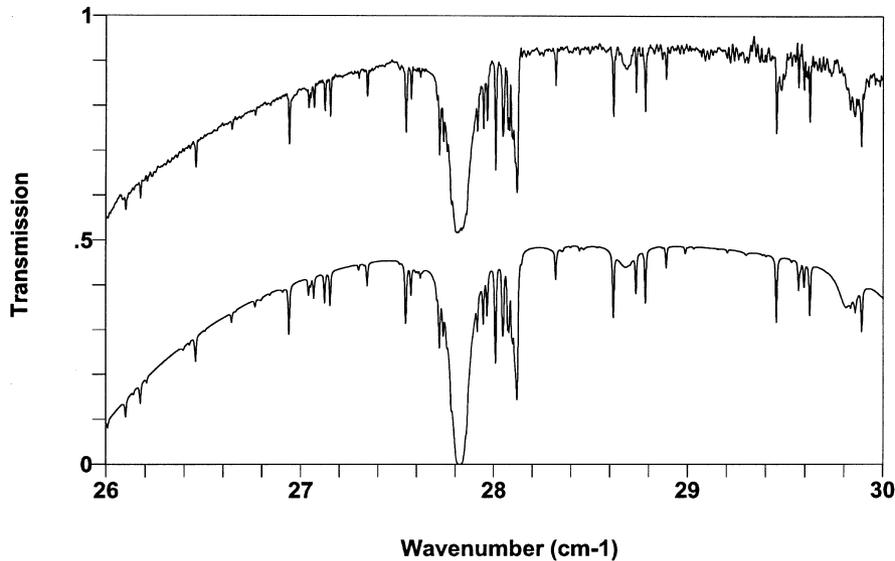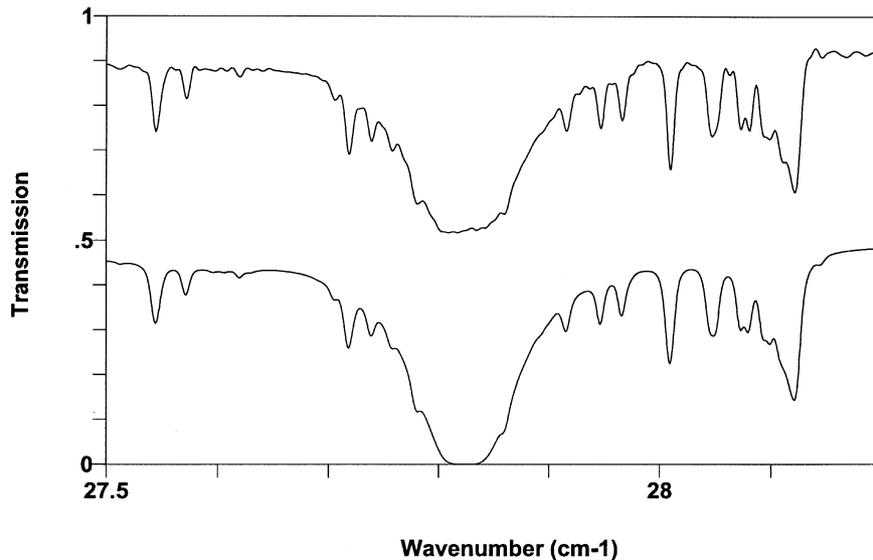
Figure 6. As Fig. 2 for the 350-μm filter band (780–900 GHz).

Figure 7. Expanded region of Fig. 6 showing detail of the agreement between the measured and model spectra (825–846 GHz).

REFERENCES

Anderson G. P. et al., 1996, in Hays P. B., Wang J., eds, Proc. SPIE Vol. 2830, Optical Spectroscopic Techniques and Instrumentation for Atmospheric and Space Research II. SPIE, Bellingham, p. 82

Chamberlin R. A., Bally J. B., 1994, Appl. Opt., 33, 1095
Clark T. A., Naylor D. A., Tompkins G. J., Duncan W. D., 1992, Sol. Phys., 140, 393
Davis G. R., 1993, J. Quant. Spectrosc. Radiat. Transfer, 50, 673
Davis G. R., Naylor D. A., Griffin M. J., Clark T. A., Holland W. S., 1997, Icarus, 130, 387
Duncan W. D., Robson E. I., Ade P. A. R., Griffin M. J., Sandell G., 1990, MNRAS, 243, 126
Forman M. L., Steel W. H., Vanasse G. A., 1966, J. Opt. Soc. Am., 56, 59
Holland W. S. et al., 1999, MNRAS, 303, 659
Lindsey C. A., Roellig T. L., 1991, ApJ, 375, 414
Matsuo H., Sakamoto A., Matsushita S., 1998, PASJ, 50, 359
Matsushita S., Matsuo H., Pardo J. R., Radford S. J. E., 1999, PASJ, 51, 603
Matthews H. E., 1999, James Clerk Maxwell Telescope Users Guide, http://www.jach.hawaii.edu
Naylor D. A., Clark T. A., 1986, in Crawford D. L., ed., Proc. SPIE Vol. 627, Instrumentation in Astronomy VI. SPIE, Bellingham, p. 482

Naylor D. A., Clark T. A., Schultz A. A., Davis G. R., 1991, MNRAS, 251, 199

Naylor D. A., Clark T. A., Davis G. R., Duncan W. D., Tompkins G. J., 1993, MNRAS, 260, 875

Naylor D. A., Clark T. A., Davis G. R., 1994a, in Crawford D. L., Craine E. R., eds, Proc. SPIE Vol. 2198, Instrumentation in Astronomy VIII. SPIE, Bellingham, p. 703

Naylor D. A., Davis G. R., Griffin M. J., Clark T. A., Gautier D., Marten A., 1994b, A&A, 291, L51

Naylor D. A., Gom B. G., Ade P. A. R., Davis J. E., 1999, Rev. Sci. Inst., 70, 4097

Rothman L. S. et al., 1998, J. Quant. Spectrosc. Radiat. Transfer, 60, 665

Serabyn E., Weisstein E. W., Lis D. C., Pardo J. R., 1998, Appl. Opt., 37, 2185

Vernazza J. E., Avrett E. H., Loeser R., 1981, ApJS, 45, 635

This paper has been typeset from a TEX/LATEX file prepared by the author.